JOURNAL OF GUIDANCE, CONTROL, AND DYNAMICS
Vol. 29, No. 5, September–October 2006

Batch Algorithm for Global-Positioning-System Attitude Determination and Integer Ambiguity Resolution

Mark L. Psiaki*
Cornell University, Ithaca, New York 14853-7501

A new algorithm has been developed for simultaneous determination of attitude and carrier phase integer ambiguities based on data from an array of global-positioning-system (GPS) antennas. The purpose of the algorithm is to reduce the required number of tracked GPS satellites and antenna baselines needed to correctly resolve the ambiguities. This new motion-based method relies on data from several sample times. The vehicle must rotate about one or more axes among the samples. The solution algorithm works in two stages. It first solves a nonlinear least-squares problem in which the single-differenced carrier-phase ambiguities are allowed to vary as continuous real numbers. The second stage solves a nonlinear least-squares problem that restricts the ambiguities to be integers. This latter algorithm uses a combined Newton/Levenberg–Marquardt method to deal with attitude quaternion nonlinearities, and it uses the least-squares ambiguity decorrelation adjustment method to deal with the integers. The second-stage algorithm is very accurate, but it needs to use initial guesses generated from first-stage algorithm solutions to find the global optimum. If the maneuver is large enough, then this new method can reliably solve difficult attitude/ambiguity-resolution problems. This capability has been demonstrated using Monte Carlo simulation. In one set of cases, the new algorithm correctly resolves ambiguities and achieves an accuracy of 4 deg or better when using two GPS satellite signals received by three antennas that are arrayed along 1-m baselines.

I. Introduction

THE global positioning system (GPS) was originally designed to determine position, velocity, and time, but its signals also can be used for attitude determination.[1–8] The most common technique for precise GPS attitude determination uses an array of antennas fixed to the vehicle whose attitude is to be determined. The carrier-phase signals from the antennas are processed to deduce the attitude of the vehicle's body-axis coordinate system measured relative to reference coordinates. The processing algorithm uses the known antenna locations in body coordinates and the known directions in reference coordinates to the GPS satellites that produced the carrier-phase signals. It operates using the principles of interferometry.[1,2,4] An alternative technique uses signal strength measurements and the receiving antennas' known gain patterns.[7]

A significant challenge in multi-antenna GPS attitude determination is the resolution of carrier cycle ambiguities. The basic attitude measurement is the phase difference between the carrier signals from a given GPS satellite as received by two different antennas. This difference consists of a known fractional part of a cycle plus an ambiguous integer number of cycles. The uncertainty in the integer part of this difference is called the integer ambiguity, and it must be determined and removed to achieve a reasonable level of attitude accuracy.

A number of researchers have developed methods for resolving the carrier cycle integer ambiguities, for example, see Refs. 1, 2, 5, and 6. These methods are aided by the fact that the ambiguities remain constant from one sample to the next if the signal strengths are strong and if the receivers are operating properly. The solution algorithms use data taken during an attitude maneuver to make the carrier cycle ambiguities observable. All such algorithms are classified as motion-based ambiguity resolution methods.

The ambiguity resolution methods of Refs. 1, 5, and 6 make various transformations and approximations to isolate subproblems. These subproblems are designed to have the attitude or the integer ambiguities drop out and to be solvable using existing algorithms. The solutions to these simpler subproblems are substituted back into the original problem as known quantities, and the original problem is solved for the remaining unknowns. Although practical, such approaches have the unfortunate effect of discarding or degrading information in the process of developing their subproblems. This feature causes the subproblems to have less observability than the original problem. As a result, the amount of GPS carrier-phase data that are required to pose sensible subproblems for ambiguity resolution is greater than the amount needed for attitude determination alone when the ambiguities are known. The method of Ref. 1 requires signals from at least four noncoplanar GPS antennas and at least three GPS satellites. The method of Refs. 5 and 6 can work with only three antennas if signals from three GPS satellites are available or with only two GPS satellites if the signals are received by four noncoplanar antennas.

Reference 2 presents a motion-based algorithm the goal of which is to enable simultaneous attitude determination and integer ambiguity resolution using as few as two GPS signals and three antennas. This is the minimum amount of data required to determine three-axis attitude when the ambiguities are already known, and it would be advantageous if this amount of data also could suffice to resolve the ambiguities. The algorithm of Ref. 2 is ad hoc and lacks convergence guarantees, but its results suggest that simultaneous attitude determination and integer ambiguity resolution can be achieved with this limited amount of data if a suitable solution algorithm can be developed. These results suggest that the requirement of some algorithms for additional data is caused by algorithm inefficiency, not by a fundamental lack of observability in the system.

The goal of the present effort is like that of Ref. 2: to develop a motion-based algorithm that solves for vehicle attitude and resolves carrier cycle ambiguities based on carrier-phase data from as few as three antennas and two satellites. The intention is to develop an algorithm that has better global convergence properties than those of Ref. 2.

This effort draws on two bodies of knowledge to achieve its goals. It uses existing nonlinear least-squares algorithms for real-valued vectors and other existing nonlinear programming techniques.[9] It also uses existing linear least-squares algorithms for mixed real and integer-valued vectors.[10]

Received 21 June 2005; revision received 27 October 2005; accepted for publication 30 October 2005.

*Associate Professor, Sibley School of Mechanical and Aerospace Engineering. Associate Fellow AIAA.

This paper makes several contributions to the field of GPS attitude determination. One is a new two-phase motion-based algorithm for the simultaneous determination of attitude and carrier-phase ambiguities using data from two or more satellites and three or more antennas. Although no proof of global convergence is given, the design of this algorithm uses methods that are tailored to produce global convergence, and test data confirm this capability. A related contribution is a demonstration that attitude and carrier-phase ambiguities are often observable simultaneously from only two satellite signals and three antennas if a sufficiently large single-axis maneuver has occurred.

Another contribution of this paper is the development of a way to use the fundamentally linear least-squares ambiguity decorrelation adjustment (LAMBDA) method for nonlinear attitude/integer-ambiguity estimation. This paper's innovation is to employ the LAMBDA method during its solution for a Newton search step. This part of a Newton optimization algorithm is equivalent to linear least squares and, therefore, is compatible with the use of a LAMBDA solver. This represents the first known use of the LAMBDA method in conjunction with constrained real-valued optimization for solving GPS attitude determination problems.

In summary, this paper's main contribution is an ability to resolve attitude and ambiguities using GPS carrier-phase measurements from the minimum number of antennas (three) and the minimum number of tracked GPS satellites (two). It achieves this by employing the LAMBDA method to simultaneously determine the attitude time history and the integer ambiguities. The algorithm of Ref. 2 is the only other known algorithm that can work with so few GPS signals and antennas, but it has poorer convergence guarantees than does this paper's new algorithm.

The remainder of this paper is organized as follows. The second section defines the motion-based attitude determination and integer ambiguity resolution problem. The third section develops the phase-I solution algorithm for the maneuver attitude time history. The fourth section presents the phase-II combined solution algorithm for the maneuver attitude time history and the carrier cycle ambiguities. The fifth section explains how multiple locally optimal solutions from the phase-I algorithm can be used to generate a set of first guesses for the phase-II algorithm. The sixth section summarizes the executive level procedure that uses the phase-I and phase-II algorithms to find the global optimal estimate by starting from multiple first guesses that produce multiple local solutions. The seventh section demonstrates the effectiveness of the new two-phase algorithm by applying it to data from a truth model simulation. The eighth section presents conclusions.

II. Attitude Determination Problem Model

A. Problem Geometry and Measurements

The geometry of carrier-phase GPS attitude determination is depicted in Fig. 1 for a typical received signal and pair of antennas. The received signal is broadcast by GPS satellite j and is received at antennas i and $I+1$, which form the ends of baseline vector $\boldsymbol{b}_i$.

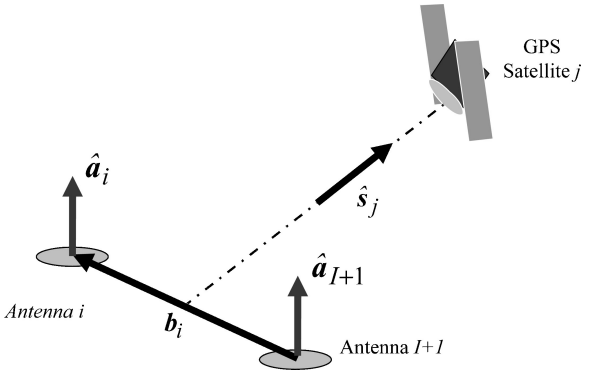

Fig. 1 Geometry of carrier-phase GPS attitude determination problem.

The total number of antennas is $I+1$. The antenna designated as $I+1$ is used as a reference to define baselines to the remaining antennas, and its carrier-phase outputs are subtracted from those of the other antennas to compute single-differenced carrier-phase measurements. The unit direction vector $\hat{\boldsymbol{s}}_j$ points along the line of sight (LOS) from the user vehicle to satellite j. The unit vectors $\hat{\boldsymbol{a}}_i$ and $\hat{\boldsymbol{a}}_{I+1}$ point along the centers of the fields of view (FOV) of antennas i and $I+1$. The vectors $\boldsymbol{b}_i, \hat{\boldsymbol{a}}_i$, and $\hat{\boldsymbol{a}}_{I+1}$ are all fixed and known in body coordinates. The vector $\hat{\boldsymbol{s}}_j$ is known in reference coordinates because the vehicle location is known from the GPS navigation solution and the satellite location is known from its broadcast ephemeredes.

Suppose that the signal-j carrier-phase measurements at antennas i and $I+1$ at sample time t_k are, respectively, $\phi_i^j(t_k)$ and $\phi_{I+1}^j(t_k)$. These measurements are given in carrier cycles. The following relationship then holds between these measurements and the geometry of Fig. 1:

$$\lambda\Delta\phi_{ijk} = \lambda\left[\phi_i^j(t_k) - \phi_{I+1}^j(t_k)\right] = -\boldsymbol{b}_i^T A(\boldsymbol{q}_k)\hat{\boldsymbol{s}}_{jk} + \lambda N_{ij} + \nu_{ijk} \tag{1}$$

where λ is the nominal carrier wavelength, $\Delta\phi_{ijk} = \phi_i^j(t_k) - \phi_{I+1}^j(t_k)$ is the computed single-differenced carrier phase for antenna baseline i and satellite j, $\boldsymbol{q}_k$ is the attitude quaternion of the vehicle body, $A(\boldsymbol{q}_k)$ is the direction cosines matrix associated with this quaternion,[11] N_{ij} is the single-differenced carrier-phase integer ambiguity for baseline i and satellite j, and ν_{ijk} is the single-differenced carrier-phase measurement noise for baseline i and satellite j. The k subscripts on the quantities $\Delta\phi_{ijk}, \boldsymbol{q}_k, \hat{\boldsymbol{s}}_{jk}$, and ν_{ijk} indicate that they apply only at sample time t_k. The integer ambiguity does not have a k subscript because it is constant over all of the samples of a maneuver if the receiver channels that track the signal from satellite j do not lose lock or experience cycle slips. (Cycle slips normally will not occur for strong signals. If they can occur, then a detection and recovery algorithm needs to be implemented that uses this paper's new algorithm with repaired carrier-phase data or with data recorded after the slip has occurred.) The unit direction vector pointing to the GPS satellite $\hat{\boldsymbol{s}}_{jk}$ is allowed to vary with time because space vehicle applications can involve a maneuver that spans a sizable fraction of the user vehicle's orbit, which will cause $\hat{\boldsymbol{s}}_{jk}$ to vary significantly during the maneuver. The attitude measurement in Eq. (1) is a cosine-type measurement; the first term on the right-hand side is the cosine of the angle between $\boldsymbol{b}_i$ and $\hat{\boldsymbol{s}}_{jk}$. This fact precludes the direct use of a QUEST-type solution, which requires vector observations.[12]

The unknowns in Eq. (1) are $\boldsymbol{q}_k$ and N_{ij}. The goal of this paper's algorithm is to estimate these quantities based on multiple versions of Eq. (1) for the baselines $i = 1, \ldots, I$; the satellites $j = 1, \ldots, J$; and the maneuver sample times $k = 1, \ldots, K$. Thus, the problem includes IJK measurement equations, K quaternion normalization constraints, and $4K + IJ$ unknowns.

Additional coarse attitude information is contained in the fact that signal j can be tracked by antennas i and $I+1$. The antennas both have limited FOVs. Tracking is possible only if the geometry of Fig. 1 obeys the inequalities

$$\hat{\boldsymbol{a}}_i^T A(\boldsymbol{q})\hat{\boldsymbol{s}}_j \geq c_{\min} \qquad \text{and} \qquad \hat{\boldsymbol{a}}_{I+1}^T A(\boldsymbol{q})\hat{\boldsymbol{s}}_j \geq c_{\min} \tag{2}$$

The lower limit $c_{\min}$ is the cosine of the maximum angle between the FOV center and the LOS vector that is required for a signal to be available. This maximum angle is about 80 to 85 deg for a typical patch antenna. The constraints in Eq. (2) constitute coarse attitude information that can be used to avoid an inverted solution.

B. Optimal Estimation Problem for Attitude Time History and Ambiguities

The single-differenced carrier phase measurements in Eq. (1) and the FOV constraints in Eq. (2) can be used to define the following

optimal estimation cost function:

$$J(\boldsymbol{q}_{\text{hist}}, \boldsymbol{N}_{\text{vec}}) = \frac{1}{2}\sum_{k=1}^{K}\sum_{j=1}^{J}\begin{bmatrix}\lambda\Delta\phi_{1jk} + \boldsymbol{b}_1^T A(\boldsymbol{q}_k)\hat{\boldsymbol{s}}_{jk} - \lambda N_{1j}\\ \vdots \\ \lambda\Delta\phi_{Ijk} + \boldsymbol{b}_I^T A(\boldsymbol{q}_k)\hat{\boldsymbol{s}}_{jk} - \lambda N_{Ij}\end{bmatrix}^T$$

$$\times R_{jk}^{-1}\begin{bmatrix}\lambda\Delta\phi_{1jk} + \boldsymbol{b}_1^T A(\boldsymbol{q}_k)\hat{\boldsymbol{s}}_{jk} - \lambda N_{1j}\\ \vdots \\ \lambda\Delta\phi_{Ijk} + \boldsymbol{b}_I^T A(\boldsymbol{q}_k)\hat{\boldsymbol{s}}_{jk} - \lambda N_{Ij}\end{bmatrix}$$

$$+\frac{1}{2}\sum_{k=1}^{K}\sum_{j=1}^{J}\sum_{i=1}^{I+1} J_{\text{pen+}}\left\{\frac{1}{\sigma_{\text{pen}}}\left[c_{\min} - \hat{\boldsymbol{a}}_i^T A(\boldsymbol{q}_k)\hat{\boldsymbol{s}}_{jk}\right]\right\} \tag{3}$$

where $\boldsymbol{q}_{\text{hist}}$ is the $(4K)$-dimensional quaternion time history vector for the K sample times and $\boldsymbol{N}_{\text{vec}}$ is the (IJ)-dimensional vector of integer ambiguities for the I baselines and J satellites:

$$\boldsymbol{q}_{\text{hist}} = \begin{bmatrix}\boldsymbol{q}_1\\ \boldsymbol{q}_2\\ \vdots\\ \boldsymbol{q}_K\end{bmatrix} \quad \text{and} \quad \boldsymbol{N}_{\text{vec}} = \begin{bmatrix}N_{11}\\ N_{21}\\ \vdots\\ N_{IJ}\end{bmatrix} \tag{4}$$

The matrix R_{jk} is the symmetric positive-definite covariance of the noise vector $[\nu_{1jk}, \ldots, \nu_{Ijk}]^T$. It has nonzero elements off of its main diagonal because each ν_{ijk} includes a common noise contribution from satellite $I+1$. The terms in the final summation of Eq. (3) penalize violations of the inequality constraints in Eq. (2) by using the one-sided penalty function:

$$J_{\text{pen+}}(\Delta c) = \begin{cases}0 & \text{if} \quad \Delta c \le 0\\ \Delta c^2 & \text{if} \quad 0 < \Delta c\end{cases} \tag{5}$$

which is depicted in Fig. 2. The penalty cost per unit of constraint violation is tuned using the positive factor $1/\sigma_{\text{pen}}$. These penalty terms only provide coarse attitude information; therefore, the optimal attitude/ambiguity solution is relatively insensitive to the value of this parameter.

The function defined in Eq. (3) is a weighted nonlinear least-squares cost function. It is weighted by the R_{jk}^{-1} matrices and by the $1/\sigma_{\text{pen}}$ parameter. It is nonlinear because the error terms that get squared are nonlinear functions of the unknown quaternions.

Given the cost function in Eq. (3) and the vector definitions in Eq. (4), the optimal estimation problem for simultaneous determination of the attitude time history and the integer ambiguities takes the form:

Find:

$$\boldsymbol{q}_{\text{hist}} \quad \text{and} \quad \boldsymbol{N}_{\text{vec}} \tag{6a}$$

To minimize:

$$J(\boldsymbol{q}_{\text{hist}}, \boldsymbol{N}_{\text{vec}}) \tag{6b}$$

Subject to:

$$\boldsymbol{q}_1^T\boldsymbol{q}_1 = \boldsymbol{q}_2^T\boldsymbol{q}_2 = \cdots = \boldsymbol{q}_K^T\boldsymbol{q}_K = 1 \tag{6c}$$

$$\text{all elements of } \boldsymbol{N}_{\text{vec}} \text{ are integers} \tag{6d}$$

This optimal estimation problem is an equality-constrained nonlinear least-squares problem with mixed real and integer unknowns. It is difficult to solve for two reasons. First, each q_k enters the problem nonlinearly. Second, the unknown ambiguities must be integers. One might be tempted to try to apply the LAMBDA method directly to this problem because the integer ambiguities enter the squared measurement error terms linearly. Unfortunately, the LAMBDA method can be applied only if all measurement errors and constraints are strictly linear in both the ambiguities and the real-valued unknowns.[10]

The foregoing analysis includes three restrictive assumptions. One is that the same antenna, antenna $I+1$, must be used to define one end of all antenna baselines for all sample times. The second assumption is that the attitude determination calculations can use a satellite's data only if they are available at all antennas for all measurement samples. The third assumption is that the antenna locations and boresight directions are fixed in body coordinates, which precludes the use of this algorithm on a highly flexible body. These assumptions are implied by the problem formulation in Eqs. (1–6d). In practice, the first two assumptions can be relaxed to the following: 1) all single-difference baselines must be linearly independent in the sense that no sum of baselines can equal another baseline and 2) a signal can be used only if it is simultaneously available from at least two antennas during at least one sample. Of course, the attitude information from a given GPS satellite and pair of antennas is improved if it is available for more than one sample, but the algorithm does not require that it be available for more than one sample. The overly restrictive versions of the first two assumptions have been used in this analysis only because they keep the already complex notation from becoming even more so.

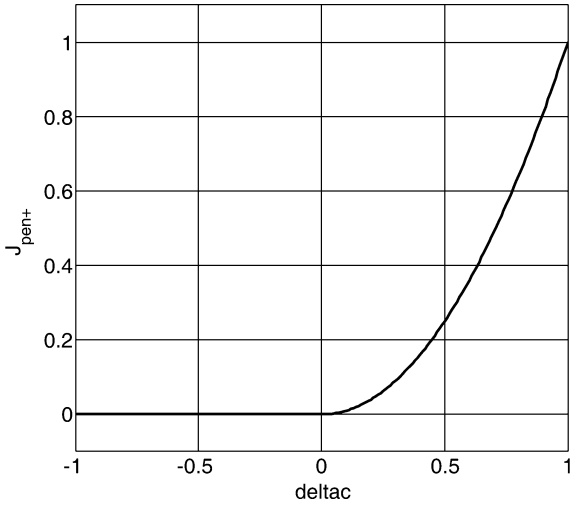

Fig. 2 Inequality constraint penalty function.

C. Transformation of Cost Function to Information Form with Decoupled Ambiguity Equations

It is useful for purposes of algorithm development to transform the cost function of Eq. (3) into a nonlinear information equation form that decouples the integer ambiguities from part of the problem and that explicitly shows the form of its dependence on the quaternion time history. The desired transformation yields the following equivalent form:

$$J(\boldsymbol{q}_{\text{hist}}, \boldsymbol{N}_{\text{vec}}) = \frac{1}{2}\sum_{l=1}^{IJ}\left(z_{Nl} - \boldsymbol{r}_{NNl}^T N_{\text{vec}} - \sum_{k=1}^{K}\boldsymbol{q}_k^T H_{Nlk}\boldsymbol{q}_k\right)^2$$

$$+\frac{1}{2}\sum_{l=1}^{IJ(K-1)}\left(z_{ql} - \sum_{k=1}^{K}\boldsymbol{q}_k^T H_{qlk}\boldsymbol{q}_k\right)^2$$

$$+\frac{1}{2}\sum_{l=1}^{(I+1)J}\sum_{k=1}^{K} J_{\text{pen+}}\left(z_{clk} - \boldsymbol{q}_k^T H_{clk}\boldsymbol{q}_k\right) \tag{7}$$

where the scalars z_{Nl} and z_{ql} are known nonhomogeneous terms in transformed carrier-phase measurement equations, the vector $\boldsymbol{r}_{NNl}^T$ is the lth row of the integer ambiguities' square, nonsingular, upper-triangular square-root information matrix R_{NN}, the symmetric 4×4 matrices H_{Nlk} and H_{qlk} are quaternion influence matrices in transformed carrier-phase equations, the scalar z_{clk} is the nonhomogeneous term in a normalized FOV inequality constraint, and the symmetric 4×4 matrix H_{clk} is the quaternion influence matrix in a normalized FOV constraint.

The derivation of the cost form in Eq. (7) from the cost form in Eq. (3) proceeds as follows: First, terms of the form $\boldsymbol{b}_i^T A(\boldsymbol{q}_k)\hat{\boldsymbol{s}}_{jk}$ are rewritten in the form $-\boldsymbol{q}_k^T H_{bijk}\boldsymbol{q}_k$, and terms of the form $\hat{\boldsymbol{a}}_i^T A(\boldsymbol{q}_k)\hat{\boldsymbol{s}}_{jk}$ are rewritten in the form $\boldsymbol{q}_k^T H_{aijk}\boldsymbol{q}_k$. This can be accomplished by using the formula for $A(\boldsymbol{q})$ from Ref. 11. Except for a possible negative sign, the resulting formula for each such H matrix is simply the formula for the q-method's K matrix with a single vector observation.[12] Second, the R_{jk} matrices are Cholesky factorized,[9] and the inverses of their Cholesky square roots are distributed to multiply the two carrier-phase error factors in the first summand of Eq. (3). This process transforms the first cost term into a sum of squares of unweighted errors of the form $(z_{eijk} - \boldsymbol{q}_k^T H_{eijk}\boldsymbol{q}_k - \boldsymbol{r}_{eijk}^T \boldsymbol{N}_{\text{vec}})$. Third, an orthonormal/upper-triangular (QR) factorization of the matrix $[\boldsymbol{r}_{e111}^T; \ldots; \boldsymbol{r}_{eIJK}^T]$ is performed to determine the square, nonsingular, upper-triangular matrix R_{NN}, as in Ref. 13, and this matrix is used to transform the z_{eijk} and H_{eijk} terms to yield the z_{Nl}, z_{ql}, H_{Nlk}, and H_{qlk} terms. Last, the quantities $c_{\min}$ and H_{aijk} are divided by σ_{pen} to yield the quantities z_{clk} and H_{clk}.

An important feature of Eq. (7) is that the ambiguities only enter the terms in the first summation. The number of terms in this summation equals the number of ambiguities, and the ambiguities enter these squared error terms linearly. The second summation in Eq. (7) is composed of squared error terms that do not depend on ambiguities. Although not apparent from the derivation of Eq. (7), these ambiguity-free terms result from time differencing of antenna-to-antenna carrier-phase single differences. Thus, the second term in Eq. (7) is a sum of squares of double-differenced carrier-phase measurement errors.

III. Phase-I Solution Algorithm That Assumes Real-Valued Ambiguities

The phase-I algorithm generates a quaternion time-history estimate for the maneuver by using standard global nonlinear optimization techniques for real-valued vectors. In cases with poor observability, this algorithm can generate a set of such estimates that define a region of reasonable time histories.

A. Elimination of Integer Ambiguities

The phase-I algorithm allows the ambiguities to be real valued, and it eliminates them from the problem by optimizing them and substituting their optimal solutions into the Eq. (7) cost function. The optimal real-valued ambiguity vector $\boldsymbol{N}_{\text{vec}}$ is computed from its first-order optimality necessary condition, which is a linear equation. The resulting formula for $\boldsymbol{N}_{\text{vec}}$ involves the inverse of the matrix $R_{NN}^T R_{NN}$ and includes terms that depend on the as-yet-unknown quaternion time history. Recall that $R_{NN} = [\boldsymbol{r}_{NN(1)}^T; \ldots; \boldsymbol{r}_{NN(IJ)}^T]$ and that it is a square, nonsingular, upper-triangular square-root information matrix; thus, $[R_{NN}^T R_{NN}]^{-1} = R_{NN}^{-1} R_{NN}^{-T}$. The notation $(\,)^{-T}$ refers to the transpose of the inverse. The remaining cost after real-valued optimization of $\boldsymbol{N}_{\text{vec}}$ consists of the last two terms in Eq. (7):

$$J_{\text{PhI}}(\boldsymbol{q}_{\text{hist}}) = \frac{1}{2}\sum_{l=1}^{IJ(K-1)}\left(z_{ql} - \sum_{k=1}^{K}\boldsymbol{q}_k^T H_{qlk}\boldsymbol{q}_k\right)^2 + \frac{1}{2}\sum_{l=1}^{(I+1)J}\sum_{k=1}^{K} J_{\text{pen}+}\left(z_{clk} - \boldsymbol{q}_k^T H_{clk}\boldsymbol{q}_k\right) \tag{8}$$

This cost function can be minimized by using standard methods for nonlinear least-squares estimation problems with real-valued unknowns. Keep in mind, however, that it is only an approximation to the cost function in Eq. (7). A significant loss of information can result from its assumption that the integer ambiguities are real valued.

B. Nonlinear Minimization Using Newton's Method

The cost function in Eq. (8) is minimized using a version of the iterative Newton procedure that has been adapted to deal with the quaternion normalization constraints in Eq. (6c). This adaptation uses ideas from the gradient projection method and from the projected Lagrangian method.[9] The phase-I algorithm proceeds as follows:

1) Start with the first guess $\boldsymbol{q}_{\text{hist}}^0$, and set the iteration counter to $n = 0$. The individual quaternion elements of this first guess must obey the normalization constraints in Eq. (6c).

2) Compute the first and second derivatives of the Eq. (8) cost with respect to $\boldsymbol{q}_{\text{hist}}$ and evaluated at the current solution guess $\boldsymbol{q}_{\text{hist}}^n$: $\boldsymbol{g}_{\text{PhI}} = (\partial J_{\text{PhI}}/\partial \boldsymbol{q}_{\text{hist}})^T$ and $H_{\text{PhI}} = \partial^2 J_{\text{PhI}}/\partial \boldsymbol{q}_{\text{hist}}^2$.

3) Compute Lagrange multipliers for the quaternion normalization constraints using the formula $\eta_k = -(\boldsymbol{q}_k^n)^T(\boldsymbol{g}_{\text{PhI}})_k$ for $k = 1, \ldots, K$, where $\boldsymbol{q}_k^n$ refers to the kth quaternion component of $\boldsymbol{q}_{\text{hist}}^n$, and $(\boldsymbol{g}_{\text{PhI}})_k$ refers to the corresponding four elements of the $\boldsymbol{g}_{\text{PhI}}$ gradient vector.

4) Use the Lagrange multipliers to compute the Hessian of the Lagrangian function:

$$\bar{H}_{\text{PhI}} = H_{\text{PhI}} + \begin{bmatrix} (\eta_1 I_{4\times 4}) & 0 & 0 \\ 0 & \ddots & 0 \\ 0 & 0 & (\eta_K I_{4\times 4}) \end{bmatrix} \tag{9}$$

5) Determine the Newton increment by solving the following optimization problem:

Find:

$$\Delta\boldsymbol{q}_{\text{hist}} \tag{10a}$$

To minimize:

$$\Delta J_{\text{PhI}} = \boldsymbol{g}_{\text{PhI}}^T \Delta\boldsymbol{q}_{\text{hist}} + \tfrac{1}{2}\Delta\boldsymbol{q}_{\text{hist}}^T\left[\bar{H}_{\text{PhI}} + \gamma I_{(4K)\times(4K)}\right]\Delta\boldsymbol{q}_{\text{hist}} \tag{10b}$$

Subject to:

$$\left(\boldsymbol{q}_1^n\right)^T \Delta\boldsymbol{q}_1 = \left(\boldsymbol{q}_2^n\right)^T \Delta\boldsymbol{q}_2 = \cdots = \left(\boldsymbol{q}_K^n\right)^T \Delta\boldsymbol{q}_K = 0 \tag{10c}$$

where $\Delta\boldsymbol{q}_k$ refers to the kth incremental quaternion component of $\Delta\boldsymbol{q}_{\text{hist}}$. This quadratic program with linear equality constraints can be solved using standard techniques provided that the projection of its Hessian onto the null space of the constraints is positive definite. The Hessian perturbation term γ is added to ensure positive definiteness. Here γ is set to zero if the projected Hessian is positive definite, but it is increased from zero to enforce positive definiteness if necessary. Use of a nonzero γ can be necessary when $\boldsymbol{q}_{\text{hist}}^n$ is remote from the solution. This modification biases the search direction $\Delta\boldsymbol{q}_{\text{hist}}$ to be more like a steepest descent direction than a Newton direction.

6) Initialize the search step length at $\alpha = 1$.

7) Compute $\boldsymbol{q}_k^{n+1} = (\boldsymbol{q}_k^n + \alpha\Delta\boldsymbol{q}_k)/[(\boldsymbol{q}_k^n + \alpha\Delta\boldsymbol{q}_k)^T(\boldsymbol{q}_k^n + \alpha\Delta\boldsymbol{q}_k)]^{0.5}$ for $k = 1, \ldots, K$, which are the quaternion components of $\boldsymbol{q}_{\text{hist}}^{n+1}$.

8) If $J_{\text{PhI}}(\boldsymbol{q}_{\text{hist}}^{n+1}) \geq J_{\text{PhI}}(\boldsymbol{q}_{\text{hist}}^n)$, then set $\alpha = \alpha/2$ and go to step 7; otherwise, go to step 9.

9) If termination criteria of the optimization are satisfied, then stop; otherwise, increment n by 1, and go to step 2.

The basic idea of all Newton procedures is to guess a solution, use Taylor-series approximation to develop a simplified problem that is valid in a neighborhood of the guessed solution, solve the simplified problem for an increment to the solution, and add that increment to the original guess. The simplified approximate problem appears in Eqs. (10a–10c), and it can be solved using matrix calculations because its first-order necessary conditions are linear in the unknowns. The line search in steps 6 through 8 reduces the length of the solution increment, if necessary, to ensure that the algorithm converges at least to a local minimum of the cost function. The algorithm maintains constraint satisfaction at each iteration by starting with a guess that is on the constraints and by using the renormalization procedure of step 7 during its line search. The Lagrange multipliers calculated in step 3 and the Hessian modification in step 4 cause the quadratic cost function approximation in Eq. (10b) to properly account for the second-order effects of the line search renormalization. The use of the nonnegative scalar γ to enforce positive definiteness

of the projected Hessian in Eq. (10b) ensures that the step-size-halving line search will terminate with a finite α that reduces the cost.

C. Global Solution Strategy and the Computation of Multiple Local Minima

It is important that the phase-I algorithm find the global minimum to the nonlinear least-squares cost function in Eq. (8). It is also important that it find any additional local minima that have a reasonably low cost, as can occur in cases of reduced observability. This latter feature is important to the generation of good first guesses for the high-accuracy phase-II algorithm.

These two goals are accomplished by multiple executions of the algorithm in steps 1–9 starting from multiple randomly chosen first guesses. Each first guess time history $\boldsymbol{q}^0_{\text{hist}}$ is generated by sampling each of its $\boldsymbol{q}^0_k$ quaternions for $k = 1, \ldots, K$ from a uniform distribution on the unit hypersphere. Uniform sampling is accomplished by first sampling an unnormalized quaternion from a four-dimensional Gaussian distribution whose mean equals zero and whose covariance equals the identity matrix. The result is then normalized to produce $\boldsymbol{q}^0_k$ (Ref. 14). This sampling procedure is performed independently for each $\boldsymbol{q}^0_k$ element of each first guess of the quaternion time history. It might be possible to generate a more efficient algorithm, that is, one that requires fewer first guesses, by including correlations between the random quaternion first guesses at neighboring sample times. The current algorithm neglects this possibility in the interest of simplicity.

The phase-I algorithm typically is run about 20 to 30 times starting from a different first guess each time. This procedure tends to produce identical solutions when the underlying attitude estimation problem has good observability, that is, when it has four or more noncoplanar antennas, three or more tracked GPS signals, and a maneuver of sufficient angular magnitude. If observability is poor, then this procedure tends to find multiple local minima. Even in this situation, it is often the case that the algorithm converges to the same local minimum from several different first guesses, but if enough first guesses are used, then there are usually several unique local minima that have a low cost and that lie in the general vicinity of the true attitude time history. One might try to increase the likelihood of finding all of the significant local minima by using more runs of the phase-I algorithm starting from more quaternion time-history first guesses, either randomly generated or chosen from some sort of grid. Computational experience with the phase-I algorithm indicates that the random first-guess method always achieves good phase-I results when seeded with 20 to 30 first guesses.

IV. Phase-II Solution Algorithm That Optimizes Attitude Time History and Integer-Valued Ambiguities

The phase-II algorithm performs an iterative minimization of the full problem cost function in Eq. (7) subject to the quaternion normalization constraints in Eq. (6c) while respecting the constraint in Eq. (6d) that the ambiguities take on integer values. This algorithm adapts the philosophy of Newton's method to the case of mixed real-valued and integer-valued unknowns. It starts with guesses of the quaternion time history $\boldsymbol{q}_{\text{hist}}$ and the ambiguity vector $\boldsymbol{N}_{\text{vec}}$, and it uses Taylor series to develop an approximate problem that is valid near the guessed solution. It solves this approximate problem for increments to the guesses, and it adds these increments to the original guesses to get an improved solution.

There are two main challenges in implementing a Newton-type method for this problem. First, the approximate problem is still a mixed real/integer optimization problem. Second, one cannot use a traditional line search to ensure global convergence because one cannot continuously vary trial increments to the ambiguity solution. The first challenge is met by employing the LAMBDA method[10] to solve the approximate problem. The second challenge is met by discarding the line search in favor of a Levenberg–Marquardt-type method of ensuring global convergence.

A. Overview of LAMBDA Solution Procedure[10]

The LAMBDA method solves integer linear least-squares problems and mixed real/integer linear least-squares problems. If the problem includes real variables, then they are optimized by solving for them from their first-order optimality necessary conditions. This solution involves a matrix inversion or some appropriate matrix factorization and produces formulas for the real variables as linear functions of the as-yet-unknown integer variables. The real variables are removed from the problem by substitution of these formulas into the original cost function. This process leaves an integer linear least-squares cost function in the following information form:

$$J_{\text{lambda}}(\Delta \boldsymbol{N}_{\text{vec}}) = \tfrac{1}{2}[\bar{R}_{NN}\Delta \boldsymbol{N}_{\text{vec}} - \bar{z}_N]^T[\bar{R}_{NN}\Delta \boldsymbol{N}_{\text{vec}} - \bar{z}_N] \quad (11)$$

where $\Delta \boldsymbol{N}_{\text{vec}}$ is the vector of unknown integers, $\bar{R}_{NN}$ is a square, nonsingular, upper-triangular square-root information matrix, and $\bar{z}_N$ is an information vector with the same dimension as $\Delta \boldsymbol{N}_{\text{vec}}$. If $\Delta \boldsymbol{N}_{\text{vec}}$ were real valued, then its optimal value would be $\bar{R}^{-1}_{NN}\bar{z}_N$.

One might be tempted to think that the optimal integer-valued $\Delta \boldsymbol{N}_{\text{vec}}$ can be found by rounding each element of the optimal real-valued solution to the nearest integer. This is usually not the case, as is illustrated by the integer optimization problem associated with Fig. 3. The optimal integer solution is $\Delta \boldsymbol{N}_{\text{vec}} = [9;5]$, which is the only point within the elliptical contour of constant cost that is shown in the figure. The real-valued optimum lies at the center of the ellipse. The four integer points nearest to this real-valued solution are $[2;-2]$, $[3;-2]$, $[3;-1]$, and $[2;-1]$. They are all remote from the true integer optimum and have a significantly higher cost than it has.

One method to determine the true optimum in Fig. 3 is to find the ellipse's bounding rectangle and do a brute-force search over all integer grid points inside it. This approach can be very inefficient if working with long, narrow hyperellipsoids in a high-dimensional space of integer ambiguities.

LAMBDA methods determine the true optimum to an integer least-squares problem using techniques that are more efficient than the bounding rectangle method. The particular method used here starts by transforming the square-root information matrix using a unimodular transformation Z on the right and an orthonormal transformation Q^T_{lambda} on the left.

$$Q^T_{\text{lambda}}\bar{R}_{NN}Z^{-1} = \tilde{R}_{NN}, \quad \Delta\tilde{\boldsymbol{N}}_{\text{vec}} = Z\Delta \boldsymbol{N}_{\text{vec}}, \quad Q^T_{\text{lambda}}\bar{z}_N = \tilde{z}_N \quad (12)$$

This transformation yields the modified, but equivalent, integer least-squares cost function

$$\tilde{J}_{\text{lambda}}(\Delta\tilde{\boldsymbol{N}}_{\text{vec}}) = \tfrac{1}{2}[\tilde{R}_{NN}\Delta\tilde{\boldsymbol{N}}_{\text{vec}} - \tilde{z}_N]^T[\tilde{R}_{NN}\Delta\tilde{\boldsymbol{N}}_{\text{vec}} - \tilde{z}_N] \quad (13)$$

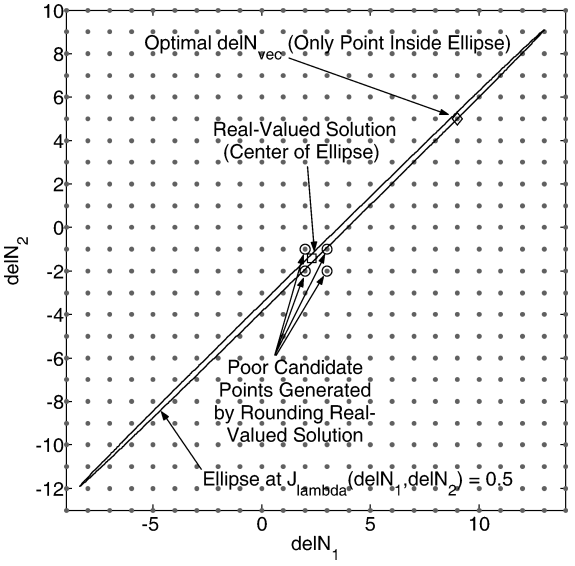

Fig. 3 Cost contour and integer grid points of an example integer least-squares problem.

The unimodular transformation Z has all integer elements, $|det(Z)|=1$, and Z^{-1} has all integer elements. These properties of Z cause an integer-valued $\Delta \boldsymbol{N}_{\text{vec}}$ to map into an integer-valued $\Delta \tilde{\boldsymbol{N}}_{\text{vec}}$ and vice versa. Therefore, restriction of the transformed unknown vector $\Delta \tilde{\boldsymbol{N}}_{\text{vec}}$ to integer values is equivalent to restriction of $\Delta \boldsymbol{N}_{\text{vec}}$ to integer values. The transformation matrices Q^T_{lambda} and Z are chosen for their ability to order the diagonal elements of the square, upper-triangular matrix $\tilde{R}_{NN}$ so that they ascend in magnitude as much as possible, or at least, so that they do not descend in magnitude too rapidly. This property serves to expedite the integer least-square solution calculations that follow.

The LAMBDA solution finishes by using modified backsubstitution procedures. Backsubstitution is an efficient means to solve an upper-triangular system of linear equations.[9] An integer form of backsubstitution is used to produce the candidate solution $\Delta \tilde{\boldsymbol{N}}_{\text{cand}}$ by performing a rounding operation after each scalar step of the real-valued backsubstitution process.[15] $\Delta \tilde{\boldsymbol{N}}_{\text{cand}}$ is often optimal if $\tilde{R}_{NN}$ has strong ascent in the magnitudes of its diagonal elements. The cost value associated with this candidate solution is used to define a hyperellipsoid in which the optimal $\Delta \tilde{\boldsymbol{N}}_{\text{vec}}$ must lie: $\tilde{J}_{\text{lambda}}(\Delta \tilde{\boldsymbol{N}}_{\text{cand}}) \geq \frac{1}{2}[\tilde{R}_{NN}\Delta \tilde{\boldsymbol{N}}_{\text{vec}} - \tilde{z}_N]^T[\tilde{R}_{NN}\Delta \tilde{\boldsymbol{N}}_{\text{vec}} - \tilde{z}_N]$. A modified set-bounding backsubstitution procedure is then used to find all values of $\Delta \tilde{\boldsymbol{N}}_{\text{vec}}$ that lie inside this ellipsoid. One of these values must be the optimum, and the algorithm finishes with a brute-force search within this set. The result is then transformed to determine $\Delta \boldsymbol{N}_{\text{vec}} = Z^{-1}\Delta \tilde{\boldsymbol{N}}_{\text{vec}}$. One can see from Fig. 3 that this method will be more efficient than the bounding rectangle method because there are many fewer integer-valued points within the figure's ellipse than are within the ellipse's bounding rectangle.

B. Phase-II Newton-Like Solution Algorithm

The steps of the phase-II algorithm are as follows:

1) Start with the first guess of the quaternion time history $\boldsymbol{q}^0_{\text{hist}}$, and set the iteration counter to $n=0$. The individual quaternion elements of this first guess must obey the normalization constraints in Eq. (6c).

2) Using the fixed value $\boldsymbol{q}^0_{\text{hist}}$, minimize the first summation term in Eq. (7) with respect to $\boldsymbol{N}_{\text{vec}}$ to compute the first-guess ambiguity vector $\boldsymbol{N}^0_{\text{vec}}$. This step is accomplished by applying the LAMBDA method.

3) Compute the first and second derivatives of the Eq. (7) cost with respect to $\boldsymbol{q}_{\text{hist}}$ and $\boldsymbol{N}_{\text{vec}}$ evaluated at the current solution guess $(\boldsymbol{q}^n_{\text{hist}},\ \boldsymbol{N}^n_{\text{vec}})$: $\boldsymbol{g}_q = (\partial J/\partial \boldsymbol{q}_{\text{hist}})^T$, $\boldsymbol{g}_N = (\partial J/\partial \boldsymbol{N}_{\text{vec}})^T$, $H_{qq} = \partial^2 J/\partial \boldsymbol{q}^2_{\text{hist}}$, $H_{qN} = \partial^2 J/\partial \boldsymbol{q}_{\text{hist}}\partial \boldsymbol{N}_{\text{vec}}$, and $H_{NN} = \partial^2 J/\partial \boldsymbol{N}^2_{\text{vec}} = R^T_{NN}R_{NN}$.

4) Compute Lagrange multipliers for the quaternion normalization constraints using the formula $\eta_k = -(\boldsymbol{q}^n_k)^T(\boldsymbol{g}_q)_k$ for $k=1,\ldots,K$.

5) Use the Lagrange multipliers to compute the Hessian of the problem's Lagrangian function with respect to $\boldsymbol{q}_{\text{hist}}$:

$$\bar{H}_{qq} = H_{qq} + \begin{bmatrix} (\eta_1 I_{4\times 4}) & 0 & 0 \\ 0 & \ddots & 0 \\ 0 & 0 & (\eta_K I_{4\times 4}) \end{bmatrix} \tag{14}$$

6) Initialize $\gamma = 0$ and $\Delta\gamma > 0$.

7) Solve the following approximation of the original optimization problem for $\Delta \boldsymbol{q}_{\text{hist}}$:

Find:

$$\Delta \boldsymbol{q}_{\text{hist}} \tag{15a}$$

To minimize:

$$\Delta J = \boldsymbol{g}^T_q \Delta \boldsymbol{q}_{\text{hist}} + \boldsymbol{g}^T_N \Delta \boldsymbol{N}_{\text{vec}} + \tfrac{1}{2}\Delta \boldsymbol{q}^T_{\text{hist}}\left[\bar{H}_{qq} + \gamma I_{(4K)\times(4K)}\right]\Delta \boldsymbol{q}_{\text{hist}} + \Delta \boldsymbol{q}^T_{\text{hist}} H_{qN}\Delta \boldsymbol{N}_{\text{vec}} + \tfrac{1}{2}\Delta \boldsymbol{N}^T_{\text{vec}} R^T_{NN} R_{NN}\Delta \boldsymbol{N}_{\text{vec}} \tag{15b}$$

Subject to:

$$\left(\boldsymbol{q}^n_1\right)^T \Delta \boldsymbol{q}_1 = \left(\boldsymbol{q}^n_2\right)^T \Delta \boldsymbol{q}_2 = \cdots = \left(\boldsymbol{q}^n_K\right)^T \Delta \boldsymbol{q}_K = 0 \tag{15c}$$

using standard linearly constrained quadratic programming techniques[9] to determine $\Delta \boldsymbol{q}_{\text{hist}}$ as a function of $\Delta \boldsymbol{N}_{\text{vec}}$. Substitute the result into the approximate cost function in Eq. (15b), and transform the resulting function using Cholesky and QR factorization[9] to yield an integer optimization problem of the form:

Find:

$$\Delta \boldsymbol{N}_{\text{vec}} \tag{16a}$$

To minimize:

$$\Delta J = \tfrac{1}{2}[\bar{R}_{NN}\Delta \boldsymbol{N}_{\text{vec}} - \bar{z}_N]^T[\bar{R}_{NN}\Delta \boldsymbol{N}_{\text{vec}} - \bar{z}_N] - \text{constant} \tag{16b}$$

Subject to:

$$\Delta \boldsymbol{N}_{\text{vec}} \text{ takes on integer values} \tag{16c}$$

During this process, it might be necessary to increase the γ perturbation to $\bar{H}_{qq}$ to ensure positive definiteness of the projected Hessian of problem (15a–15c).

8) Solve problem (16a–16c) using the LAMBDA method, and use this result to determine $\Delta \boldsymbol{q}_{\text{hist}}$ from the solution of problem (15a–15c).

9) Compute $\boldsymbol{q}^{n+1}_k = (\boldsymbol{q}^n_k + \Delta \boldsymbol{q}_k)/[(\boldsymbol{q}^n_k + \Delta \boldsymbol{q}_k)^T(\boldsymbol{q}^n_k + \Delta \boldsymbol{q}_k)]^{0.5}$ for $k=1,\ldots,K$ to form $\boldsymbol{q}^{n+1}_{\text{hist}}$ and compute $\boldsymbol{N}^{n+1}_{\text{vec}} = N^n_{\text{vec}} + \Delta \boldsymbol{N}_{\text{vec}}$.

10) If $J(\boldsymbol{q}^{n+1}_{\text{hist}}, \boldsymbol{N}^{n+1}_{\text{vec}}) \geq J(\boldsymbol{q}^n_{\text{hist}}, \boldsymbol{N}^n_{\text{vec}})$, then set $\gamma = \gamma + \Delta\gamma$ and $\Delta\gamma = 4\Delta\gamma$, and go to step 7; otherwise, go to step 11.

11) If termination criteria of the optimization are satisfied, then stop; otherwise, increment n by 1, and go to step 3.

This algorithm is similar to the phase-I algorithm in spirit and in form, but there are three important distinctions. First, this algorithm solves for increments to both $\Delta \boldsymbol{q}_{\text{hist}}$ and $\Delta \boldsymbol{N}_{\text{vec}}$. Second, this solution procedure happens in two stages. The stage in step 7 computes the optimal $\Delta \boldsymbol{q}_{\text{hist}}$ as a function of $\Delta \boldsymbol{N}_{\text{vec}}$ via standard techniques, and it uses this relationship to eliminate $\Delta \boldsymbol{q}_{\text{hist}}$ from the problem. The stage in step 8 uses the LAMBDA method to determined the optimal integer-valued $\Delta \boldsymbol{N}_{\text{vec}}$, and this solution is used to determine the optimal $\Delta \boldsymbol{q}_{\text{hist}}$.

The third distinction is that the phase-II algorithm ensures that a cost decrease occurs by using increments to the Levenberg–Marquardt parameter γ instead of a line search. It is straightforward to show that the γ iteration in steps 7–10 will terminate with a cost decrease after a finite number of iterations. This technique applies a "soft" limit to the magnitude of $\Delta \boldsymbol{q}_{\text{hist}}$ in cases where the cost decrement test in step 10 fails. It places no restrictions on the magnitude of $\Delta \boldsymbol{N}_{\text{vec}}$ because $\boldsymbol{N}_{\text{vec}}$ enters the Eq. (7) cost quadratically, which implies that the cost function in Eq. (15b) is exact for pure $\Delta \boldsymbol{N}_{\text{vec}}$ variations. This technique allows the LAMBDA solution in step 8 to maintain integer $\Delta \boldsymbol{N}_{\text{vec}}$ values while the magnitude of $\Delta \boldsymbol{q}_{\text{hist}}$ decreases in a line-search-like process.

The phase-II algorithm is guaranteed to converge at least to a local minimum of the problem in Eqs. (6a–6d). The cost decrease enforced by steps 7–10 ensures that the algorithm makes progress towards a local minimum if it is not already at one. A local minimum in this mixed real/integer optimization problem is a point with a cost that is lower than all other possible solutions whose $\boldsymbol{q}_{\text{hist}}$ values lie in some small neighborhood of the locally minimizing $\boldsymbol{q}_{\text{hist}}$ but whose $\boldsymbol{N}_{\text{vec}}$ values are free to vary without limit.

The partial solution procedure for problem (15a–15c) can be used to compute the estimator's quaternion time-history covariance matrix. This computation projects the Hessian matrix $\bar{H}_{qq}$ into the null space of the Eq. (15c) constraints, inverts the projected Hessian, and maps the result back to the full space. The resulting covariance matrix has K eigenvalues that equal zero, one along the direction of each quaternion. This is consistent with the fact that the linearized normalization constraint implies perfect knowledge of the quaternion in this direction.

This algorithm has the option of computing only an approximate H_{qq} in step 3. The Gauss–Newton approximation is used in this case; it only employs the squared Jacobian part of H_{qq}. This approximate H_{qq} is less costly to compute; it guarantees positive definiteness of the projected Hessian in problem (15a–15c) even when $\gamma = 0$, and

it yields a convergence rate that is equivalent to the rate of the full Newton method if the optimal measurement residuals are small.[9]

V. Synthesis of Random Phase-II Initial Guesses from Multiple Phase-I Local Minima

The phase-II algorithm needs to start with a good first guess to find the global minimum of the cost in Eq. (7) subject to the constraints in Eqs. (6c) and (6d). The phase-II algorithm is only guaranteed to converge to a local minimum. The presence of integer unknowns in this problem tends to increase the number of local minima. Therefore, it is necessary to start near the global minimum to find it using the phase-II algorithm. The strategy for starting with a good first guess is to execute the phase-II algorithm multiple times starting from randomized first guesses that have a tendency to lie near the global minimum.

The approach for seeding the phase-II algorithm is to use solutions from the phase-I algorithm. If problem observability is strong, then there is usually a single solution for all of the phase-I first guesses, and it constitutes a very good first guess for the phase-II algorithm. In other situations, the phase-I algorithm tends to produce multiple distinct local solutions that have low-cost values.

The situation of poor observability is depicted in Fig. 4 on a three-dimensional projection of one of the $\boldsymbol{q}_k$ hyperspheres. Three distinct phase-I local minima occur in the lightly shaded region of the sphere. The lightly shaded region corresponds to low phase-I cost and high phase-I a posterior probability. This figure illustrates how the problem's weak observability makes the phase-I algorithm a poor means of estimating the attitude. There are many possible $\boldsymbol{q}_k$ values that are highly consistent with the transformed phase-I measurements, that is, all of the values in the lightly shaded region. It is impossible to distinguish the true attitude from among these many possible solutions by means of phase-I cost alone.

The local minima of a phase-I solution can be used to synthesize good first guesses for the phase-II algorithm even when none of them constitutes an accurate solution itself. Consider on Fig. 4 the spherical triangle whose vertices are the three phase-I local minima. This triangle bounds a region in which there is a high probability of finding the global solution to the phase-II problem.

The procedure for generating phase-II initial guesses is to randomly produce convex combinations of phase-I local solutions. Suppose that the distinct phase-I solutions are $\boldsymbol{q}_{\text{hist}}^{PhI(m)}$ for $m = 1, \ldots, M_{\text{PhI}}$, where M_{PhI} is the number of distinct local minima. Suppose that the solution for $m = 1$ has the lowest cost. Then the signs of the quaternion components of the solutions for $m = 2, \ldots, M_{\text{PhI}}$ are reversed, as needed, to enforce $[\boldsymbol{q}_{\text{hist}}^{PhI(1)}]^T \boldsymbol{q}_{\text{hist}}^{PhI(m)} \geq 0$. Next, unnormalized probability weights are computed for the phase-I solutions by using the formula

$$p(m) = \exp\left\{-J_{\text{PhI}}\left[\boldsymbol{q}_{\text{hist}}^{PhI(m)}\right]\right\} \qquad \text{for} \qquad m = 1, \ldots, M_{\text{PhI}} \tag{17}$$

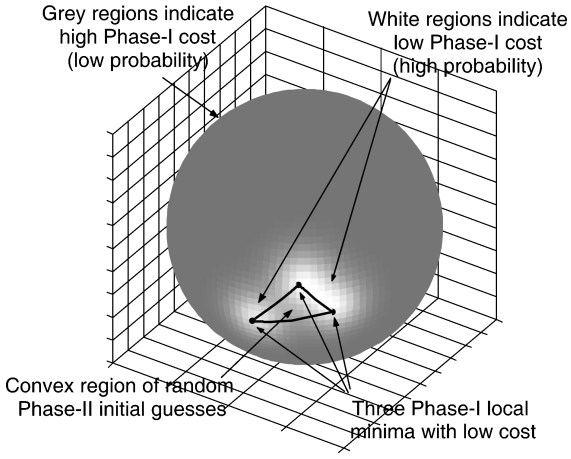

Fig. 4 Three-dimensional illustration of probabilities and local minima associated with phase-I costs, a case with poor observability.

Given these weights, the following procedure is used to compute each random first guess for the phase-II algorithm. Independent random samples are drawn from a uniform distribution over the range [0,1], $s(m) \sim U[0,1]$ for $m = 1, \ldots, M_{\text{PhI}}$, and these random samples are combined with the probability weights of Eq. (17) to produce the following convex combination coefficients:

$$\beta(m) = \frac{p(m)s(m)}{\sum_{n=1}^{M_{PhI}} p(n)s(n)} \qquad \text{for} \qquad m = 1, \ldots, M_{\text{PhI}} \tag{18}$$

These coefficients all lie in the range $0 \leq \beta(m) \leq 1$, and they sum to 1. They are used to form a convex combination of the phase-I local minima using the formulas

$$\boldsymbol{q}_{\text{histun}} = \sum_{m=1}^{M_{PhI}} \beta(m) \boldsymbol{q}_{\text{hist}}^{PhI(m)} \quad \text{and}$$

$$\boldsymbol{q}_k^0 = \frac{\boldsymbol{q}_{\text{unk}}}{\sqrt{\boldsymbol{q}_{\text{unk}}^T \boldsymbol{q}_{\text{unk}}}} \quad \text{for} \quad k = 1, \ldots, K \tag{19}$$

where $\boldsymbol{q}_{\text{unk}}$ is the unnormalized kth quaternion in the $\boldsymbol{q}_{\text{histun}}$ time history and where $\boldsymbol{q}_k^0$ is the corresponding normalized quaternion in the phase-II first guess time history $\boldsymbol{q}_{\text{hist}}^0$.

Equation (19) forms $\boldsymbol{q}_{\text{hist}}^0$ as the normalized equivalent of $\boldsymbol{q}_{\text{histun}}$, which is a random convex combination of the phase-I local minima. Lower-cost minima have larger $\beta(m)$ coefficients in the convex sum, on average. This property places the phase-II first guesses closer to the lower-cost phase-I local minima, on average. In the Fig. 4 example, each convex combination is sampled randomly from the interior of the spherical triangle that connects the three phase-I local minima.

VI. Integration of Phase-I and Phase-II Algorithms

This paper's approach to doing combined attitude determination and ambiguity resolution requires that its phase-I and phase-II algorithms be integrated into an executive procedure. This procedure runs both algorithms multiple times from multiple random first guesses, it uses outputs of the phase-I algorithm to generate the phase-II first guesses, and it sorts through multiple solutions from the phase-II algorithm to determine the global minimum. Suppose that the executive procedure has been instructed to generate M_1 phase-I solutions starting from independent random first guesses and to generate M_2 phase-II solutions starting from additional random first guesses. The executive procedure operates as follows:

1) Generate M_1 random attitude time-history guesses $\boldsymbol{q}_{\text{hist}}^{PhI0(m)}$ for $m = 1, \ldots, M_1$ by using the uniform quaternion sampling method described near the end of this paper's third section and in Ref. 14.

2) Run the phase-I algorithm M_1 times starting from the independent first guesses of step 1 to solve for the phase-I solutions $\boldsymbol{q}_{\text{hist}}^{PhIs(m)}$ for $m = 1, \ldots, M_1$.

3) Delete from the set $\{\boldsymbol{q}_{\text{hist}}^{PhIs(1)}, \ldots, \boldsymbol{q}_{\text{hist}}^{PhIs(M_1)}\}$ all redundant local minima to create the set $\{\boldsymbol{q}_{\text{hist}}^{PhI(1)}, \ldots, q_{\text{hist}}^{PhI(M_{PhI})}\}$, and perform quaternion sign reversals, as needed, to match the signs of the quaternions in the phase-I global minimum. Each element of the original solution set is equivalent to an element of this new set, but the elements of the new set obey $\boldsymbol{q}_{\text{hist}}^{PhI(m)} \neq \boldsymbol{q}_{\text{hist}}^{PhI(n)}$ for all $m \neq n$ in the range 1 to M_{PhI}. The number of independent phase-I solutions $M_{\text{PhI}} \leq M_1$ is determined by this deletion procedure.

4) Use the set of unique phase-I solutions $\{\boldsymbol{q}_{\text{hist}}^{PhI(1)}, \ldots, \boldsymbol{q}_{\text{hist}}^{PhI(M_{PhI})}\}$ and the sampling calculations in Eqs. (17–19) to generate a total of M_2 random attitude time-history guesses $\boldsymbol{q}_{\text{hist}}^{PhII0(m)}$ for $m = 1, \ldots, M_2$.

5) Run the phase-II algorithm M_2 times starting from the independent first guesses of step 4 to solve for the phase-II solutions $[\boldsymbol{q}_{\text{hist}}^{PhII(m)}, N_{\text{vec}}^{PhII(m)}]$ for $m = 1, \ldots, M_2$.

6) Find the phase-II solution that has the lowest cost, that is, find $[\boldsymbol{q}_{\text{hist}}^{PhII(n)}, \boldsymbol{N}_{\text{vec}}^{PhII(n)}]$ such that $J[\boldsymbol{q}_{\text{hist}}^{PhII(n)}, \boldsymbol{N}_{\text{vec}}^{PhII(n)}] \leq J[\boldsymbol{q}_{\text{hist}}^{PhII(m)}, \boldsymbol{N}_{\text{vec}}^{PhII(m)}]$ for all $m = 1, \ldots, M_2$. This quaternion time history and ambiguity vector constitute this algorithm's best solution of problem (6a–6d).

This executive procedure tends to produce the true global minimum in the limit of large M_1 and M_2. Practical example calculations indicate that the required numbers of independent first guesses and solutions are on the order of $M_1 = 20$ to 30 and $M_2 = 30$ to 60. Values in these ranges seem to produce sets of first guesses that have sufficient geometric diversity to guarantee global convergence. These conclusions are based on computational experience. Further investigation is required to determine the best choices for M_1 and M_2.

This batch algorithm represents a first-cut attempt to solve the combined GPS attitude determination/integer ambiguity resolution problem using data from only two satellites and three antennas. It uses a batch approach because that is the easiest to implement. It might be possible to generate an equally effective recursive filtered version of the algorithm, as is done in Refs. 5 and 6, but any such development must await a future research project and paper.

VII. Algorithm Performance on Example Cases

A. Truth-Model Simulation

A simulation has been used to generate data for use in testing this paper's new algorithms. The simulation is given truth values for the single-differenced integer ambiguities, N_{ij} for $i = 1, \ldots, I$ and $j = 1, \ldots, J$, and it is given a truth quaternion time history that corresponds to an attitude maneuver $\boldsymbol{q}_k$ for $k = 1, \ldots, K$. It uses these truth quantities to generate simulated carrier-phase measurement data using the formulas

$$\lambda\phi_i^j(t_k) = -\boldsymbol{r}_i^T A(\boldsymbol{q}_k)\hat{\boldsymbol{s}}_{jk} + \mu_{jk} + \lambda N_{ij} + \nu_{ijk}$$

$$\text{for} \quad i = 1, \ldots, I, \qquad j = 1, \ldots, J, \qquad \text{and} \qquad k = 1, \ldots, K \tag{20a}$$

$$\lambda\phi_{I+1}^j(t_k) = -\boldsymbol{r}_{I+1}^T A(\boldsymbol{q}_k)\hat{\boldsymbol{s}}_{jk} + \mu_{jk} + \nu_{(I+1)jk}$$

$$\text{for} \qquad j = 1, \ldots, J \qquad \text{and} \qquad k = 1, \ldots, K \tag{20b}$$

where $\boldsymbol{r}_i$ is the position vector of antenna i measured in body coordinates, μ_{jk} is the real-valued carrier-phase ambiguity for antenna $I+1$ and GPS satellite j at sample time t_k, and ν_{ijk} is the carrier-phase noise for antenna i and satellite j at sample time t_k. The noise is generated as the sum of two components. One component comes from a Gaussian random number generator with a mean of zero and a standard deviation of 0.00025 m or less; it reflects the expected thermal noise error at a carrier-to-noise ratio of $C/N_0 = 48.7$ dB-Hz and a phase-lock loop bandwidth of 10 Hz. The other noise component models multipath error. Most cases model it as being a function of the user-vehicle-referenced vector that points to the GPS satellite $A(\boldsymbol{q}_k)\hat{\boldsymbol{s}}_{jk}$. This model uses an independent randomly generated 12th-order/12th-degree spherical harmonic expansion with a peak value of 0.015 m for each GPS antenna's multipath error, which yields a peak error in the single-differenced carrier phase of 0.03 m. Each antenna's multipath model is held fixed for all sample times, which preserves the spatial correlation of this error source. Phase measurements are generated for a particular antenna/satellite pair only if the corresponding Eq. (2) FOV constraint is satisfied. The carrier wavelength $\lambda = 0.1903$ m has been used, which corresponds to the GPS L1 signal.

Equation (1) uses single differencing, but Eqs. (20a) and (20b) are raw, undifferenced carrier-phase equations. Undifferenced carrier-phase simulation provides a convenient means of properly modeling the correlated noise that occurs in single-differenced measurements, but it requires the use of the additional real-valued ambiguity μ_{jk} to produce realistic outputs. The single-differenced baselines associated with this model are $\boldsymbol{b}_i = \boldsymbol{r}_i - \boldsymbol{r}_{I+1}$ for $i = 1, \ldots, I$. Simulated single-differenced measurements are computed for these baselines by differencing the simulated raw-phase data that are produced by Eqs. (20a) and (20b). This differencing causes μ_{jk} to drop out of the simulation's outputs.

The truth integer ambiguities, N_{ij} for $i = 1, \ldots, I$ and $j = 1, \ldots, J$, have been chosen to lie in the range $-100{,}000 \le N_{ij} \le 100{,}000$. This range is wide enough to fully exercise the solution algorithm. These are simulated as exact integer values. This simulation presumes that electrical line biases have been calibrated and removed from the single-differenced carrier-phase measurements. If this were not the case, then the single-differenced ambiguities would not be integers, and this paper's algorithm would have to be modified to use double differences rather than single differences to produce integer ambiguities.

B. Summary of Cases and Results

A number of test cases have been considered, and multiple Monte Carlo simulation runs have been performed for many of these cases. Two types of maneuvers have been considered. One is the pitch rotation of a nadir-pointing satellite in low Earth orbit (LEO). The other is a yaw maneuver of a taxiing airplane. Several combinations of the numbers of antennas, satellites, and measurement samples have been considered ranging from $I + 1 =$ three to four antennas (i.e., $I =$ two to three baselines), $J =$ two to four satellites, and $K =$ four to six samples per maneuver. Antenna baseline lengths have ranged from 1 m up to 6.4 m to cover a range of typical vehicles that include spacecraft and small aircraft. Typical numbers of random first guesses and algorithm executions are $M_1 = 20$ to 60 for phase I and $M_2 = 30$ to 60 for phase II.

The two-phase algorithm performed well in all reasonable cases. A number of cases with only three antennas and two satellite signals have been considered, and the new algorithm has achieved accurate global solutions in all cases that have good observability. Peak total attitude errors of less then 5 deg have been achieved in these cases with antenna baselines ranging from 1 to 1.5 m, and the integer ambiguities have been resolved correctly.

The only cases that have given poor results are cases with only three antennas, only two satellites, short antenna baselines (on the order of 1 m), small angular separations between the two satellites, and small attitude maneuvers. Such cases have poor observability. The global minimum of the Eq. (7) cost function can have incorrect ambiguities and an inaccurate attitude time-history estimate. Alternatively, the global minimum can be accurate, but its cost value might be nearly indistinguishable from that of a local minimum whose ambiguities are wrong and whose attitude is inaccurate. This type of behavior does not represent a deficiency of the two-phase algorithm; rather, it represents an observability deficiency of the original problem.

C. Two Representative Examples

The results from two representative examples serve to illustrate the performance of the algorithm. The first example involves a LEO satellite whose three zenith-pointing antennas form two 1-meter baselines at right angles to each other. The satellite orbit is nearly circular at an altitude of 600 km and an inclination of 28 deg. Its three antennas receive signals from two GPS satellites. The natural pitch motion of this nadir-pointing satellite provides the maneuver necessary for determining the integer ambiguities.

The two-phase algorithm successfully resolves the integer ambiguities and determines the attitude time history to an accuracy of 1.7 deg or better if it uses six samples spread out evenly over a quarter of an orbit, that is, over 25 min during which a 93.1-deg pitch rotation occurs. This case's accurate global minimum of the phase-II problem is clearly distinguishable as the best solution. Figure 5 demonstrates the uniqueness of the global solution by plotting the maximum total error of each local solution's estimated attitude time history vs the solution's Eq. (7) cost. The global minimum cost is 28.5 times smaller than the cost of the next best local minimum, and its peak attitude error is 20.4 times smaller than that of the local solution with the next lowest cost.

The good results of this case are dependent on the magnitude of the attitude variation during the maneuver. The new algorithm has resolved the ambiguities correctly and produced attitude estimates that are accurate to 4 deg or better in 202 of 202 Monte Carlo simulation runs with 93.1 deg of pitch motion and in 101 of 102 Monte Carlo runs with 74.5 deg of motion, but it has failed to resolve the ambiguities correctly in 1 of 102 runs with 74.5 deg of pitch motion and in 18 of 102 runs with 55.8 deg of motion. Thus, a decrease of

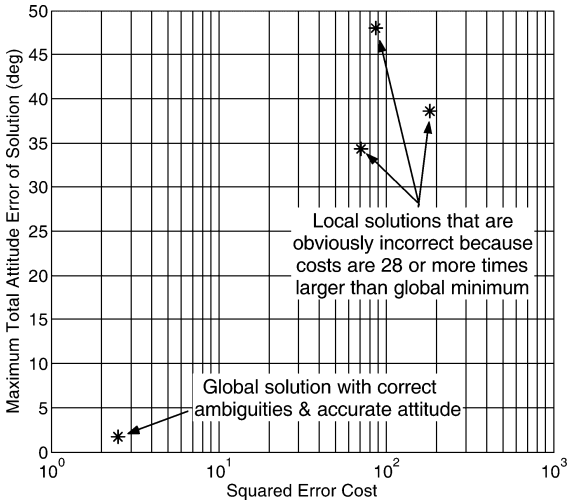

Fig. 5 Maximum total attitude error vs phase-II solution cost for a LEO satellite that rotates 93.1 deg in pitch.

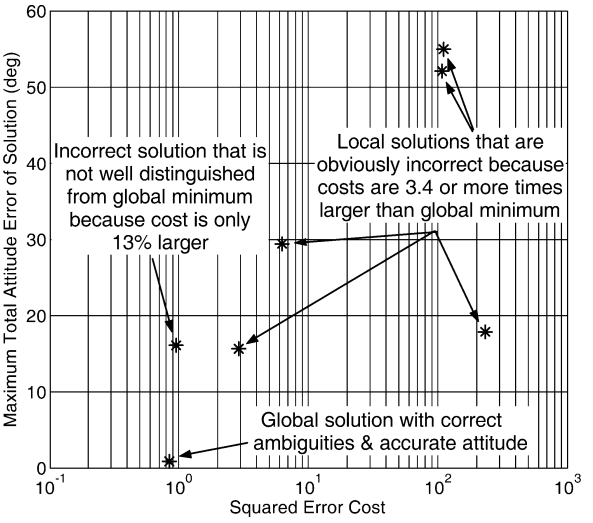

Fig. 6 Maximum total attitude error vs phase-II solution cost for a taxiing aircraft that rotates 90 deg in yaw.

the maneuver magnitude weakens the system's observability. The way to get good results for a short maneuver is to add more data. If a third satellite is available, then good observability can be had from only 5 min worth of data, during which the pitch rotation is only 18.6 deg. The global phase-II solution yields worst-case attitude errors of 2.6 deg under these conditions.

A factor that affects observability is the separation between the two tracked GPS satellites. The minimum, maximum, and average angular separations between the LOS vectors to the two tracked GPS satellites associated with Fig. 5 are, respectively, 61.5, 87.5, and 78.9 deg. If a different pair of satellites is chosen that has less angular separation, then observability is reduced. Monte Carlo simulations have been run for a pair of satellites with minimum, maximum, and average angular separations of 36.2, 45.3, and 42.5 deg, respectively, and with the same pitch maneuver of 93.1 deg. Of 202 Monte Carlo simulation runs for this case, 132 have global phase-II solutions that resolve the ambiguities incorrectly and that yield very inaccurate attitude estimates.

The second example case is that of an airplane executing a yaw maneuver on a runway prior to takeoff. Its three zenith-pointing antennas form two perpendicular baselines each of length 1.5 m, and the antennas track only two GPS satellites. If the yaw maneuver is 180 deg, then the observability is good. The phase-II algorithm has resolved the ambiguities correctly and has achieved peak total attitude errors of 5 deg or less in all 202 Monte Carlo simulations that have been run for this case. These runs have used randomized directions to the two tracked GPS satellites to produce satellite angular separations ranging from 30 to 150 deg.

If the aircraft's yaw maneuver only spans 90 deg, however, then the observability is reduced. The phase-II global solution yields incorrect ambiguities and inaccurate attitude estimates in 12 of 202 Monte Carlo runs. Furthermore, some cases that yield an accurate global minimum do not have a very distinct minimum. Consider Fig. 6, which plots the maximum total attitude error vs the solution cost for the unique phase-II local solutions, similar to Fig. 5, for one of the 202 Monte Carlo simulation runs. The solution with the global minimum cost yields the correct ambiguities and an attitude accuracy of better than 1 deg, but this solution is not well distinguished from another that has only 13% more cost. This second solution resolves the ambiguities incorrectly, and its peak total attitude error is more than 16 deg. This dubious result is not the fault of the new algorithm. Rather, it is the fault of the poor observability of the actual system, which is caused by the limited maneuver angle. The only way to ensure against this problem is to increase observability by using techniques that are discussed next.

D. Performance Trends

Certain trends have emerged from the cases that have been considered. The most important trends are those that affect observability. Observability tends to improve as antenna baselines get longer, as angular separations between the tracked GPS satellite LOS vectors increase and as the angular magnitude of the maneuver increases. Observability also improves with increases in the number of antennas or the number of tracked satellites. Improvements in observability increase the likelihood of correct ambiguity resolution and reduce estimation error magnitudes. They also tend to reduce the number of distinct local minima and the number of random first guesses and algorithm executions that are required to find the global minimum.

The phase-II algorithm yields better accuracy than the phase-I algorithm if the underlying problem has a moderate level of observability. It does this by computing a global solution with a lower Eq. (7) cost than that achieved by the phase-I algorithm after modification of its real ambiguities into "nearby" integers. For example, consider the LEO satellite case associated with Fig. 5. The global minimum of the phase-I algorithm has a 6.6-deg peak total attitude error, but the phase-II algorithm's global minimum has a peak error of only 1.7 deg. This happens because the phase-II algorithm improves its estimates by using more information than the phase-I algorithm. The additional information is the knowledge that the ambiguities are integers rather than real numbers, and this represents a nontrivial amount of information in certain situations. Note, however, that the phase-I algorithm can achieve good accuracy in cases where strong observability is provided by data from three or more satellites, four or more noncoplanar antennas, and a large maneuver.

The phase-II algorithm's LAMBDA procedure has a demonstrated ability to modify the $\boldsymbol{N}_{\text{vec}}$ ambiguities vector to reduce the estimation error cost function. This feature allows it to correct ambiguity errors as part of its estimation process. The phase-II algorithm does not require a first guess of the attitude time history that yields the true ambiguities during its step 2 initialization. It can correct residual ambiguity errors during its step 8 LAMBDA iterations. Note, however, that the minimization procedure does not always produce movement from incorrect ambiguities to the correct ones. Cases have been recorded where step 2 of the phase-II algorithm initializes the ambiguities at their correct values, but the step 8 iterations move the ambiguity estimates away from these values. This can happen if the initial quaternion time-history guess is too far from the optimal solution. In all cases, however, the phase-II iterations reduce the Eq. (7) cost. This seemingly perverse behavior can be tolerated in cases of reasonable observability. It will cause the ambiguity accuracy to degrade for some solutions, but other solutions will resolve the ambiguities correctly and produce the global minimum cost along with accurate attitude estimates.

E. Execution Speed

The new two-phase algorithm has been tested in MATLAB® running in interpretive mode on a 3.0-GHz processor. CPU times per

solution ranged from 31 to 166 s for problems with $I+1=$ three to four antennas, $J=$ two to four GPS satellites, and $K=$ four to six samples. The execution time tends to increase sharply with increases in the number of samples K. Solutions that used $K=$ four samples had a mean execution time of 44 s, but solutions that used $K=$ six samples had a mean execution time of 126 s. The total execution time varies nearly linearly with M_1, the number of phase-I solutions, but it is less sensitive to M_2, the number of phase-II solutions, because phase II tends to terminate in fewer iterations. The execution time is also relatively insensitive to the number of ambiguities that need to be resolved. This counterintuitive result probably stems from the fact that an increased number of ambiguities corresponds to an increased amount of data, which makes the original phase-I solutions more accurate. Phase II requires only a few iterations in such cases.

These execution times imply that the new algorithm would be practical for one-time batch startup calculations using an embedded microprocessor. The use of a small embedded microprocessor would tend to slow execution in comparison to the current results, but the use of compiled software rather than interpretive software would tend to recoup some of the lost speed. The algorithm only needs to execute during a cold start. A simpler recursive Kalman filter can take over the task of real-time attitude determination after the ambiguities have been correctly resolved. In the spacecraft application, the initial batch solution would operate on data that were collected over 1500 s of orbit, and it would execute in about 170 s or less; thus, it could execute in a timely manner for attitude filter initialization.

This paper's new two-phase algorithm has been compared with a brute-force algorithm to determine its relative solution speed. The latter algorithm considers all possible N_{ij} ambiguity values that could satisfy Eq. (1) for all possible attitudes. This involves the derivation of minimum and maximum N_{ij} limits. These are determined by using the minimum and maximum limits on the first term on the right-hand side of Eq. (1), $-\|\boldsymbol{b}_i\|$ and $+\|\boldsymbol{b}_i\|$, and by setting conservative lower and upper limits for the noise term in Eq. (1) at -6 and $+6$ times its standard deviation. Suppose that $N_{\text{ij min}}$ is the greatest lower bound on N_{ij} maximized over all $k=1,\ldots,K$ and that N_{ijmax} is the least upper bound minimized over the same k values. All possible integer combinations in the range $N_{\text{ij min}} \le N_{ij} \le N_{\text{ij max}}$ for $i=1,\ldots,I$ and $j=1,\ldots,J$ are tried, and the original cost function in Eq. (3) is minimized by independently optimizing each $\boldsymbol{q}_k$ for $k=1,\ldots,K$. Each $\boldsymbol{q}_k$ nonlinear least-squares optimization starts from four random initial guesses on the unit hypersphere to ensure that the global minimum is determined. The cost is summed over all sample times for each combination of the ambiguities, and the combination that gives the lowest overall cost is chosen as the best estimate.

This paper's new algorithm has been compared with the brute-force algorithm for two sets of example cases. One set of cases uses three antennas that are arranged in two perpendicular 1-m baselines. The four ambiguities of these cases might be expected to produce a total of $(2/.19)^4 \cong 12{,}277$ brute-force search cases, but the actual measurements limit the number of cases to only 1584. The brute-force algorithm requires 3.19 times as much CPU time, on average, to solve these cases than does the this paper's new algorithm when the latter method uses $M_1=30$ phase-I first guesses and $M_2=45$ phase-II first guesses. The other set of cases expands the two perpendicular antenna baselines to a length of 1.5 m, and the brute-force algorithm's number of possible integer ambiguity combinations expands to 4725. The brute-force algorithm uses an average of 17.9 times as much CPU time as does this paper's new algorithm for these problems when the new algorithm uses phase-I and phase-II first guesses that number, respectively, $M_1=20$ and $M_2=30$. Thus, the new algorithm is significantly faster than the brute-force algorithm for small antenna baselines, and its relative speed advantage grows as the antenna baseline length grows.

VIII. Conclusions

A two-phase motion-based algorithm has been developed to simultaneously solve for attitude and integer ambiguities using GPS single-differenced carrier-phase data from an array of antennas. The algorithm minimizes the sum of weighted squared measurement errors and penalty terms that enforce "soft" visibility constraints. The algorithm's first phase treats the carrier cycle ambiguities as real numbers and solves for rough attitude time-history estimates. Its second phase treats the ambiguities as exact integers and uses a combination of Newton's method and the Levenberg–Marquardt method to deal with the nonlinearities along with the LAMBDA method to deal with the integers.

The algorithm includes heuristic procedures that tend to give it reliable global convergence. These involve multiple solutions starting from multiple random first guesses of the attitude time history. The guesses for the first phase are distributed as uniform random attitudes. The guesses for the second phase are randomized convex combinations of the locally optimal attitude time histories that have been determined during the first phase.

The two-phase algorithm retains all attitude information, including the integer nature of the cycle ambiguities. The treatment of ambiguities as integers forces the algorithm to be complex, but enables it to estimate the attitude accurately in situations of reduced data availability. Given a sufficiently large maneuver, the algorithm can resolve the ambiguities and achieve peak attitude errors of 4 deg or less with only two GPS satellite signals and two 1-m antenna baselines. An example of an adequate maneuver is the 90-deg quarter-orbit rotation of a nadir-pointing LEO satellite.

References

[1]Cohen, C. E., "Attitude Determination," *Global Positioning System: Theory and Applications*, Vol. II, edited by B. W. Parkinson and J. J. Spilker, Jr., AIAA, Reston, VA, 1996, pp. 519–538.

[2]Conway, A., Montgomery, P., Rock, S., Cannon, R., and Parkinson, B., "A New Motion-Based Algorithm for GPS Attitude Integer Resolution," *Navigation*, Vol. 43, No. 2, Summer 1996, pp. 179–190.

[3]Axelrad, P., and Behre, C. P., "Attitude Estimation Algorithms for Spinning Satellites Using Global Positioning System Phase Data," *Journal of Guidance, Control, and Dynamics*, Vol. 20, No. 1, 1997, pp. 164–169.

[4]Crassidis, J. L., Lightsey, E. G., and Markley, F. L., "Efficient and Optimal Attitude Determination Using Recursive Global Positioning System Signal Operations," *Journal of Guidance, Control, and Dynamics*, Vol. 22, No. 2, 1999, pp. 193–201.

[5]Crassidis, J. L., Markley, F. L., and Lightsey, E. G., "Global Positioning System Integer Ambiguity Resolution Without Attitude Knowledge," *Journal of Guidance, Control, and Dynamics*, Vol. 22, No. 2, 1999, pp. 212–218.

[6]Lightsey, E. G., and Crassidis, J. L., "Real Time Attitude Independent GPS Integer Ambiguity Resolution," *Advances in the Astronautical Sciences, Proceedings of the John L. Junkins Astronautics Symposium*, Vol. 115, edited by S. R. Vadali and D. Mortari, Univelt, Inc., San Diego, CA, 2003, pp. 145–163.

[7]Lightsey, E. G., and Madsen, J., "Three-Axis Attitude Determination Using Global Positioning System Signal Strength Measurements," *Journal of Guidance, Control, and Dynamics*, Vol. 26, No. 2, 2003, pp. 304–310.

[8]Jung, H., Psiaki, M. L., Scott, W. J., and Boitnott, C. L., "Attitude Sensing Using a GPS Antenna on a Turntable, Experimental Tests," *Navigation*, Vol. 51, No. 3, Fall 2004, pp. 221–229.

[9]Gill, P. E., Murray, W., and Wright, M. H., *Practical Optimization*, Academic Press, New York, 1981, pp. 31, 36–40, 88–93, 99–115, 133–141, 162–164, 219–224, 233–247.

[10]Teunissen, P. J. G., "The Least-Squares Ambiguity Decorrelation Adjustment: A Method for Fast GPS Integer Ambiguity Estimation," *Journal of Geodesy*, Vol. 70, Nos. 1–2, Nov. 1995, pp. 65–82.

[11]Wertz, J. R. (ed.), *Spacecraft Attitude Determination and Control*, D. Reidel, Boston, 1978, pp. 414–416.

[12]Shuster, M. D., "In QUEST of Better Attitudes," *Advances in the Astronautical Sciences*, Vol. 108, Dec. 2001, pp. 2089–2117.

[13]Bierman, G. J., *Factorization Methods for Discrete Sequential Estimation*, Academic Press, New York, 1977, pp. 69–76, 115–122.

[14]Shuster, M. D., "Uniform Attitude Probability Distributions," *Journal of the Astronautical Sciences*, Vol. 51, No. 4, 2003, pp. 451–475.

[15]Psiaki, M. L., and Mohiuddin, S., "GPS Integer Ambiguity Resolution Using Factorized Least-Squares Techniques," *Proceedings of the Flight Mechanics Symposium*, edited by J. K. Thienel, NASA CP-2005-212789, NASA, Greenbelt, MD, 2005.